

Initial stages of epitaxial CoSi_2 formation on $\text{Si}(100)$ surfaces

G. Rangelov, P. Augustin, J. Stober, and Th. Fauster

Sektion Physik, Universität München, Schellingstraße 4, 80799 München, Germany

(Received 5 May 1993; revised manuscript received 29 November 1993)

The initial stages of the CoSi_2 formation on $\text{Si}(100)$ surfaces after room-temperature Co deposition and subsequent annealing were studied using Auger electron spectroscopy, low-energy electron diffraction, and valence-band and core-level photoemission spectroscopy with synchrotron radiation. CoSi_2 formation does not take place at room temperature. A coverage dependence of the reaction temperature on $\text{Si}(100)$ is observed which is attributed to a change of the Co adsorption sites at room temperature above a Co coverage of ~ 2.5 monolayer. This is related to the formation of CoSi_2 grains and of pinholes. Co-rich and Si-rich CoSi_2 surfaces were observed and characterized for different annealing temperatures. A Si termination of the Co-rich surface is inferred from our data. A $c(4 \times 4)$ reconstruction of the Si-rich surface is observed.

I. INTRODUCTION

Silicides have been studied extensively in the past decade due to their importance as conducting materials in microelectronics. CoSi_2 has the advantage that it grows epitaxially on Si (lattice mismatch $\sim -1.2\%$) which opens prospects for three-dimensional electronic devices. Up to now CoSi_2 formation on $\text{Si}(111)$ has been usually studied experimentally (for a recent review, see Ref. 1), and high-quality epitaxial films have been grown. However, $\text{CoSi}_2(100)$ is technologically more relevant and in the last few years many studies have appeared.²⁻⁹ In contrast to growth on $\text{Si}(111)$, however, grains of CoSi_2 with different orientations grow on the $\text{Si}(100)$ surface after annealing of Co films deposited at room temperature (RT).^{2,3,5} Therefore, a template technique is used to grow films with a single orientation.^{2,3} Such a template is formed from the deposition of ~ 2.6 Å Co at RT, followed by the deposition of several angstroms of Co and Si in stoichiometric ratio and further annealing to 460°C .³ Obviously, it is quite important to understand the very first stages of CoSi_2 formation on $\text{Si}(100)$ after RT Co deposition.

Gallego *et al.*⁶ concluded from their Auger electron spectroscopy (AES) and photoemission data that CoSi_2 forms for $\theta_{\text{Co}} < 1$ ML. At higher coverages a Co-Si mixture grows in a layer-by-layer mode. AES and surface extended x-ray-absorption fine-structure measurements⁷ showed that one can distinguish between several stages of the interface formation at RT. For $\theta_{\text{Co}} < 0.5$ ML, Co atoms chemisorb on the $\text{Si}(100)$ surface, occupying fourfold sites. For $0.5 \text{ ML} < \theta_{\text{Co}} < 2.5$ ML, the Co atoms diffuse into the lattice, occupying interstitial sites. Above 2.5 ML, substitution of the Si host atoms by Co takes place. In contrast to Gallego *et al.*⁶ the authors of Ref. 7 exclude a spontaneous CoSi_2 formation on $\text{Si}(100)$ at RT. To some extent the disagreement between different authors may be due to slightly different preparation procedures and experimental conditions.

Another important problem is the surface termination

of the silicide layer. In contrast to $\text{CoSi}_2(111)$,¹⁰ the termination of the $\text{CoSi}_2(100)$ surface is not clear at all. Gallego *et al.*⁶ concluded from their AES and oxygen titration experiments that a Co-rich Si-terminated CoSi_2 -C surface appears after annealing to 250°C . Further annealing to 600°C leads to a Si-rich CoSi_2 -S surface. After annealing to 460°C of Co films deposited at RT Chambless *et al.*⁸ observed a $c(2 \times 2)$ LEED (low-energy electron diffraction) pattern and attributed it to the surface reconstruction of the CoSi_2 -C film terminated with 0.5 ML of Co atoms. In a recent scanning-tunneling-microscopy study Stalder *et al.*⁹ claim that the $c(2 \times 2)$ surface is Si terminated, in agreement with Gallego *et al.*⁶ These authors studied the $\text{CoSi}_2(100)$ -S surface as well and observed two different reconstructions: another $c(2 \times 2)$ and a $(3\sqrt{2} \times \sqrt{2})R45^\circ$ structure. A (2×2) structure was observed during the transition between the two reconstructions.

We have studied CoSi_2 formation using a variety of surface-sensitive techniques: AES, LEED, and valence-band and core-level spectroscopy with synchrotron radiation. AES was mainly used to control the Co coverage and compare to values reported in the literature for the various surface terminations. LEED indicates the crystallographic order of the surfaces and helps to identify the reconstructions characteristic for differently terminated surfaces. The valence-band spectra give a picture of the electronic structure of the surface and are used to monitor the silicide formation. The highly surface-sensitive Si $2p$ core-level spectra reflect the bonding configuration of the Si atoms and allow an easy identification of contributions from CoSi_2 and Co-Si in solid solution. Similar information is obtained from Co $3p$ core-level spectra.

II. EXPERIMENT

The experiments were performed in an ultrahigh-vacuum apparatus consisting of a preparation and an analyzer chamber. The preparation chamber¹¹ is equipped

with standard LEED optics, a cylindrical mirror analyzer for AES, a quadrupole mass spectrometer, evaporation sources, and a quartz microbalance for thickness measurements. The photoemission experiments have been performed at the TGM-3 (toroidal grating monochromator) beamline at the BESSY (Berliner-Elektronenspeicherring-Gesellschaft für Synchrotronstrahlung) storage ring. The emitted electrons were detected by means of a display-type electron-energy spectrometer¹² housed in the analyzer chamber. The overall resolution of the analyzer and the monochromator for 130-eV photon energy and ~ 30 eV kinetic energy was ~ 0.35 eV. The large acceptance angle of the spectrometer ($\sim 88^\circ$) allowed for true angular integration and for fast data accumulation with good statistics. The typical measuring times were ~ 10 min at a base pressure of $\sim 4 \times 10^{-11}$ mbar. The measured counting rates were normalized to the photon flux, so an absolute comparison between the intensities of different spectra is possible.

The boron-doped Si crystals ($\sim 5 \Omega\text{cm}$) were Ar^+ sputtered ($10 \mu\text{A}$, 600 eV), annealed to 850°C , and slowly cooled down ($\sim 1\text{--}2^\circ\text{C/s}$) to room temperature. The crystals were directly heated and their temperature above 460°C was measured by an infrared pyrometer. Below 460°C the temperature was determined from the heating power, which has been calibrated in a separate experiment with a thermocouple attached to the crystal. Co and Si were evaporated on the samples held at room temperature using a liquid-nitrogen-cooled electron-beam evaporator. The base pressure during the evaporation was $\sim 5 \times 10^{-10}$ mbar. The evaporated amount was determined by means of the quartz microbalance. Typical evaporation rates were $\sim 0.5\text{--}1$ ML/min. The microbalance reading was compared to the AES and LEED uptake behavior. In the case of Co on Si(100) the Si/(Si+Co) AES signal versus the Co coverage θ_{Co} estimated by the quartz microbalance is shown in Fig. 1. The AES ratio decreases linearly up to ~ 2.5 ML. At higher Co coverages the linear decrease continues with a smaller slope. This behavior is identical to the one observed by Meyerheim, Döbler, and Puschmann⁷ who

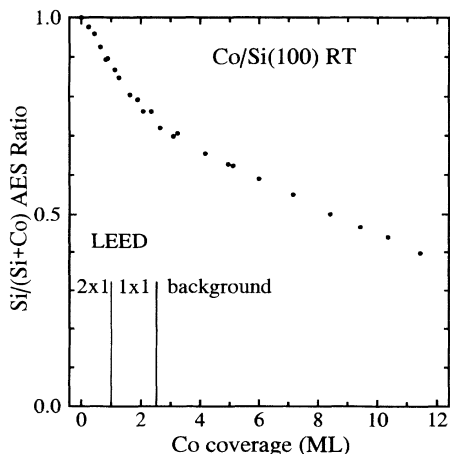


FIG. 1. Co uptake on Si(100) at room temperature monitored by AES and LEED.

performed an absolute coverage calibration by Rutherford backscattering (RBS). The change of the LEED pattern as a function of the Co coverage is also indicated in Fig. 1. The half-order spots of the clean surface (2×1) structure disappear for coverages above 1 ML and the (1×1) spots disappear at $\theta_{\text{Co}} > 2.5$ ML, in agreement with Ref. 7. Therefore, our coverage calibration coincides with the absolute calibration by RBS.⁷ There is one more point concerning the Si(100) surface preparation which it is worthwhile to discuss here. Meyerheim, Döbler, and Puschmann⁷ compare in their study the Co uptake on Ar^+ -sputtered and HF-etched Si(100) surfaces, discovering pronounced differences in the growth mode due to surface roughening after Ar^+ sputtering. Our AES and LEED uptake data are nearly identical to their data for HF-etched surfaces. Therefore, we conclude that our cleaning procedure does not influence the Co growth as dramatically as their Ar^+ -sputtering ($1\text{--}1.5$ keV) followed by annealing to 800°C . It should be mentioned that we also changed the crystals after several experiments.

III. AUGER ELECTRON SPECTROSCOPY AND LEED

The AES and LEED uptake behavior at RT is shown in Fig. 1 and has been discussed briefly in Sec. II. The annealing of the Co films evaporated at RT leads to a reduction of the Co signal, the effect being stronger for higher Co coverages. Our results (not shown) for the Co AES signal versus annealing temperature at different θ_{Co} are similar to those shown by Gallego *et al.*⁶ For $\theta_{\text{Co}} > 4$ ML and at 460°C ($550\text{--}650^\circ\text{C}$) we obtained a Co/Si AES ratio of 0.18 (0.07), $\sim 25\%$ smaller than that for the $\text{CoSi}_2\text{-C}$ ($\text{CoSi}_2\text{-S}$) layer on a Si(111) surface.¹⁰ This difference could be due to pinholes in our films or to a lower thickness of our films ($\leq 10 \text{ \AA}$) so that the substrate can contribute to the total Si AES signal (mean free path $\sim 5 \text{ \AA}$ for the Si *L*VV electrons).⁷ Like Gallego *et al.*⁶ we interpret this as the formation of Co-rich and of Si-rich CoSi_2 surfaces.

We observed several LEED patterns after the annealing of Co films on the Si(100) surface. They are summarized in Fig. 2. For θ_{Co} around 1 ML the (1×1) structure is stable to $\sim 550^\circ\text{C}$. At higher temperatures and for coverages lower than 2 ML the (2×1) structure, typical for the clean Si(100), surface reappears. The same effect was observed by Meyerheim, Döbler, and Puschmann.⁷ At ~ 5 ML Co we observe above 420°C a $c(2 \times 2)$ structure as mentioned before.^{13,14} For higher coverages this structure appears at higher temperatures (see Fig. 2). At the best quality of the $c(2 \times 2)$ structure the spots are slightly brighter than those of the clean surface, which means that the areas covered with this structure are comparable to the LEED coherence length of $\sim 100 \text{ \AA}$. This structure has been attributed to a reconstruction of the CoSi_2 overlayer which is terminated either with 0.5 ML Co (Ref. 13) or 1 ML Si.⁹ Further annealing of the $c(2 \times 2)$ [also called the $(\sqrt{2} \times \sqrt{2})R45^\circ$] structure to temperatures above $\sim 600^\circ\text{C}$ leads to the appearance of a $c(4 \times 4)$ [also

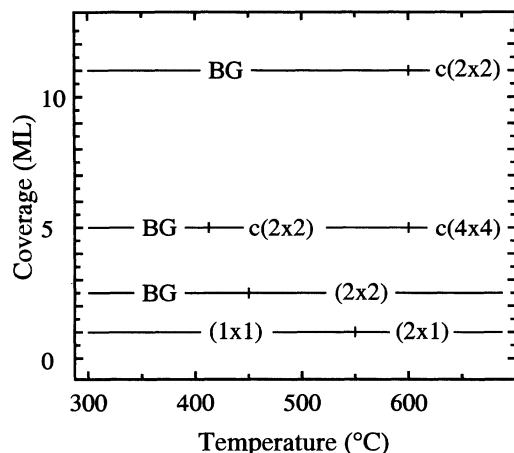


FIG. 2. LEED patterns observed on Si(100) as a function of temperature and Co precoverage. The absence of ordered structures is denoted by BG (background).

called $(2\sqrt{2} \times 2\sqrt{2})R45^\circ$] structure not reported before to our knowledge. This structure appears with its best quality (comparable to the clean surface) and at even lower temperature of $\sim 550^\circ\text{C}$ if sandwich films of stoichiometric ratio are evaporated on a Co layer of $\sim 2\text{--}3$ ML. We assign this structure to the Si-rich CoSi₂-S surface termination characterized above by AES.

For Co coverages around 2.5 ML (where at RT no LEED pattern exists) we observed above $\sim 450^\circ\text{C}$ a $p(2 \times 2)$ structure, which we attribute to a mixture of the (2×1) and the $c(2 \times 2)$ structures. Clean Si(100) patches (pinholes) and $c(2 \times 2)$ reconstructed CoSi₂ islands with dimensions close the LEED coherence length (100 \AA) could be a possible explanation. Using only AES and LEED data we cannot exclude, however, the possibility that pinholes exist at Co coverages where only the $c(2 \times 2)$ or $c(4 \times 4)$ structures appear. If they exist, their diameter should be considerably smaller than the LEED

coherence length. It should be added that we never observed the $(3\sqrt{2} \times \sqrt{2})R45^\circ$ structure reported by Stalder *et al.*⁹

IV. VALENCE-BAND PHOTOEMISSION

We followed the silicide formation after annealing the RT Co films. Figure 3 contains the valence-band spectra for $\theta_{\text{Co}} = 0.7$ ML and 5 ML taken at 115 eV photon energy in the angle-integrated mode of the display spectrometer. This means that we recorded a cross-section-weighted density of states (DOS) and we can compare our spectra to the calculated DOS. At this photon energy the states with Co $3d$ character dominate the spectra.¹⁵ It is well known¹⁶ that two main peaks exist in the CoSi₂ DOS: Co $3d$ nonbonding states at ~ 1.7 eV below the Fermi level (E_F) and a Co $3d$ -Si $3p$ bonding combination at ~ -3.7 eV. The spectrum of the clean Si(100)- (2×1) surface is shown in Fig. 3(a) for comparison. The 0.7-ML RT spectrum has a broad peak with a maximum at ~ 1 eV below E_F . This means that most of the Co atoms have not reacted to CoSi₂ in contrast to the statement of Gallego *et al.*⁶ Annealing to 300°C causes almost no changes in the spectrum [Fig. 3(a)]. A weak shoulder appears on the left side of the peak, where the Co $3d$ nonbonding states for CoSi₂ are expected. At 460°C the spectrum intensity decreases, the peak maximum shifts to ~ -1.7 eV as in CoSi₂, but the peak is broader and contains a shoulder at ~ -1 eV, the RT peak position, corresponding to lower-coordinated Co atoms. The data suggest that up to 460°C the CoSi₂ formation reaction is not complete and some Co atoms are not surrounded by eight Si atoms as in CoSi₂. After the 650°C anneal we observe an additional intensity decrease and the peak shape resembles that of the CoSi₂ DOS.¹⁷ This suggests that at low Co coverages (similar spectra were observed for $\theta_{\text{Co}} = 1.3$ ML, not shown) and high-temperature annealing three-dimensional CoSi₂ islands covered with Si exist on the Si(100) surface. At ~ -4 eV a pronounced

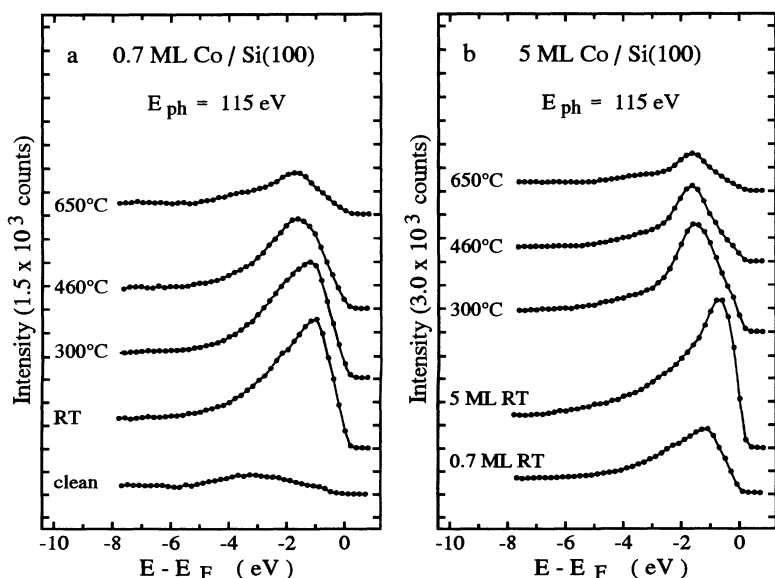


FIG. 3. Co/Si(100), valence-band spectra (a) for $\theta_{\text{Co}} = 0.7$ ML and (b) for $\theta_{\text{Co}} = 5$ ML. The intensity units correspond to the distance between two axes markers.

shoulder is seen, where the Co 3*d*-Si 3*p* bonding peak is expected. The relative intensity of the shoulder in comparison to the CoSi₂ spectrum suggests that some contribution from the Si patches is also possible (compare to the bottom spectrum).

Figure 3(b) presents the results of the analogous experiment for 5 ML Co/Si(100). The bottom spectrum for 0.7 ML of Co deposited at RT is shown for comparison. The peak maximum of the 5-ML spectrum at RT is shifted further to higher energy at ~ -0.7 eV as expected if an unreacted Co film grows on the surface. The annealing to 300 °C shifts the peak maximum to ~ -1.7 eV, the value for stoichiometric CoSi₂. The peak is asymmetric at the right side which means that not all Co atoms have identical surroundings. Further annealing to 460 °C leads to a valence-band spectrum identical to that of CoSi₂. Annealing to 650 °C does not change the peak form but causes an intensity decrease. One can attribute this effect to a Si overlayer covering the CoSi₂ layer. It should be noted that for 2.6 ML Co/Si(100) we observed a similar behavior.

To summarize, from our valence-band experiments we can conclude that no complete reaction to CoSi₂ takes place at room temperature even for the lowest coverages studied here (0.7 ML). Annealing is necessary for CoSi₂ formation. At $\theta_{\text{Co}} \geq 2.5$ ML annealing to ~ 460 °C is enough for CoSi₂ formation, but for lower coverages we obtain the CoSi₂ DOS only after annealing at ~ 650 °C. Si-rich CoSi₂-S overlayers are formed after high-temperature annealing (> 460 °C). Islands of CoSi₂ exist on the surface at least for very low θ_{Co} .

V. Si 2*p* CORE-LEVEL SPECTRA

The data-evaluation procedure for the core-level spectra will be demonstrated for the clean Si(100)-(2 × 1) surface. Figure 4 shows a Si 2*p* spectrum (dots) taken at 130 eV photon energy. The spectra are normalized to the photon flux, and therefore an absolute comparison of the intensities is possible. The Si 2*p* electrons are emitted with a kinetic energy of ~ 30 eV having a mean free path of ~ 3.3 Å.¹⁸ The Si 2*p* spectra were fitted by means of a least-squares fit procedure using the Levenberg-Marquardt method.¹⁹ For the peak form Doniach-Sunjić²⁰ functions convoluted with a Gaussian broadening function were used. The Gaussian reflects the experimental energy resolution (monochromator and electron analyzer) which is ~ 0.35 eV. The branching ratio of the Si 2*p*_{3/2} and 2*p*_{1/2} components (0.5), their separation (0.608 eV), the Lorentzian full width at half maximum (FWHM) (0.08 eV)^{21,22} and the asymmetry parameter^{20,23} were kept constant. In the case of the clean Si(100) surface the asymmetry parameter was set to zero.¹⁸ For the Si 2*p* spectra of silicides the asymmetry parameter was set to 0.12.^{22,24} The background was fitted by a third-order polynomial plus the contribution from inelastically scattered electrons proportional to the integral of the elastic peak. The solid line through the data is the fit function resulting from the fit. The background is shown by the dashed line. Three main Si

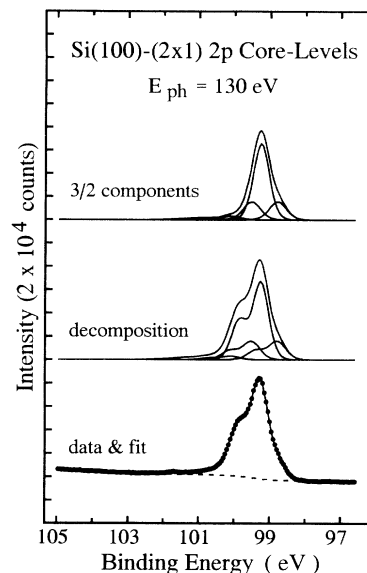


FIG. 4. Si(100) Si 2*p* spectrum, bottom: original data and fit function, center: peak decomposition and top: 2*p*_{3/2} components. The intensity units correspond to the distance between two axes markers.

2*p* components were needed for the best fit. They are shown in the center of Fig. 4 together with the fit function. The existence of different Si 2*p* components is due to binding-energy shifts of the Si 2*p* levels of Si atoms in a chemical environment different from that in bulk Si.¹⁸ The most intensive component is due to emission from Si bulk atoms. Both equally intense components on both sides of the bulk peak originate from the Si surface atoms, which are lower coordinated than the bulk atoms and have unsaturated bonds (dangling bonds). To reduce the number of the dangling bonds, asymmetric dimers forming the Si(100)-(2 × 1) reconstructed surface appear.¹⁸ The right component is from the negatively charged outer dimer atoms and the left one is from the positively charged inner dimer atoms. Their intensities correspond to half a monolayer each.¹⁸ Due to the excellent statistic ($\sim 100\,000$ counts/channel maximum) and to the quality of the fit we will not show the experimental points but only the fit functions. For clarity only the Si 2*p*_{3/2} components of the peaks will be shown (Fig. 4, top).

Figure 5 presents the Si 2*p*_{3/2} spectra for 1.3 ML and 5 ML on Co/Si(100) as functions of the annealing temperature. The bottom spectra are for the clean Si(100)-(2 × 1) surface with its three components discussed above. The Co adsorption leads to a reduction of the total intensity due to the screening effect of the Co film and to a slight shift of the 2*p* manifold to lower binding energy (0.15 eV) due to band-bending effects, and removes the surface contribution due to dangling-bond saturation. We estimate the Schottky barrier height to be 0.40 ± 0.02 eV, in agreement with Refs. 6 and 25. We observe that a new component grows with Co coverage. The binding-energy shift (-0.28 eV) of this peak corresponds to that observed for the Co-Si solid solution^{26,27} on Si(111). According to the thermodynamical treatment of the core-level shifts

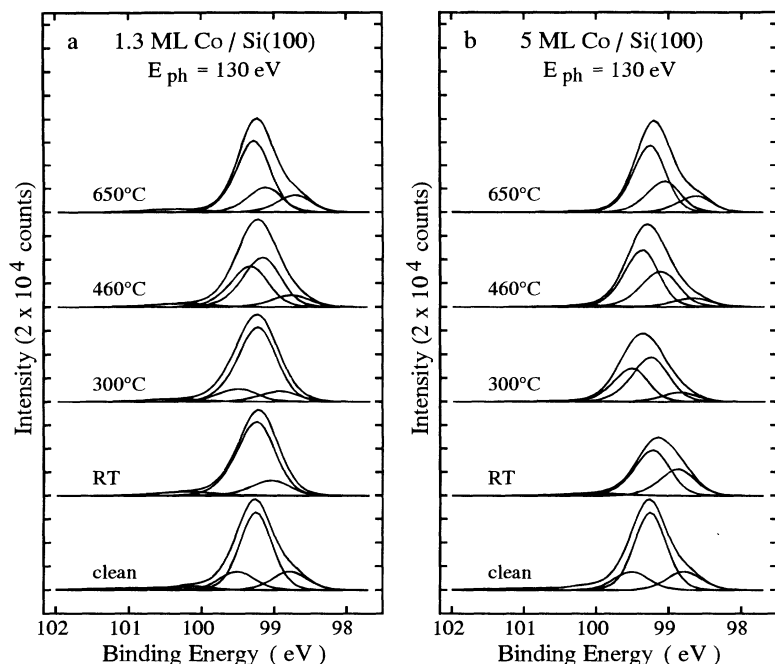


FIG. 5. Co/Si(100), Si $2p_{3/2}$ component (a) for $\theta_{\text{Co}} = 1.3$ ML and (b) for $\theta_{\text{Co}} = 5$ ML. The intensity units correspond to the distance between two axes markers.

in silicides, one should not expect an orientation dependence of the shifts.²⁸ Therefore, we attribute this peak to emission from Si atoms in Co-Si solid solution. It should be mentioned that Boscherini *et al.*²⁶ observed an additional peak (with binding-energy shift of ~ 0.36 eV) which they attributed to Si atoms in a CoSi₂-like environment. We did not observe emission from a CoSi₂-like phase and, therefore, we exclude its formation at RT. Our sensitivity allows us to detect ~ 0.1 ML of Si atoms in this phase.

Additional annealing to 300 °C was needed to get a peak shifted to higher binding energy which we attribute to CoSi₂ on the Si(100) surface. Its binding energy coincides with that on Si(111).^{26,27} From Fig. 5(a) we see that after annealing to 300 °C we do not observe a substantial contribution from CoSi₂ in the Si $2p$ spectrum for $\theta_{\text{Co}} = 1.3$ ML. On the other hand, for $\theta_{\text{Co}} = 5$ ML we do observe an intensive component due to CoSi₂. The CoSi₂ components grow mainly at the expense of the Co-Si and Si bulk components, which lose their intensity. The effect is much more pronounced for $\theta_{\text{Co}} > 2.5$ ML. Simultaneously, a shift of the right peak to lower binding energy occurs. The shift is again most pronounced for $\theta_{\text{Co}} > 2.5$ ML. For these coverages the binding-energy shift reaches ~ -0.42 eV relative to the Si bulk line. Simultaneously, the total Si $2p$ intensity increases, demonstrating once more that the reaction has taken place. After annealing to 460 °C, the CoSi₂ components for both coverages increase at the expense of the Si bulk component, the effect for the 1.3-ML film being much stronger. Therefore, for $\theta_{\text{Co}} < 2.5$ ML annealing to ~ 460 °C is needed for reaction. For $\theta_{\text{Co}} > 2.5$ ML the intensity and binding energy of the right component do not change. For lower coverages, however, an additional binding-energy shift occurs and the binding energy of the right component reaches the value it has for the higher coverages. This effect supports the above statement that for $\theta_{\text{Co}} < 2.5$ ML the

reaction to CoSi₂ needs an annealing to ~ 460 °C. We see that for all coverages the RT Co-Si converts to disilicide after annealing. Nevertheless, a component shifted to lower binding energy relative to the bulk line exists. Such a component could be due to emission from lower-coordinated surface Si atoms, similar to surface emission from the upper dimer atoms of the clean Si(2×1) surface. The binding-energy difference between the CoSi₂ peak and the right component is ~ -0.62 eV, in agreement with the data for a CoSi₂(100) single crystal (-0.61 eV).²⁹ Let us remember that after annealing to 460 °C the CoSi₂-C surface forms. The fact that we observe a surface contribution in the Si $2p$ spectra of this surface allows us to conclude that the surface is Si terminated. We can rule out the Co termination of the surface proposed by Chambliss *et al.*¹³ because in this case all dangling bonds of the surface would be saturated and no low-coordinated Si atoms would exist. Thus our conclusions are in agreement with the statement of Stalder *et al.*⁹

Further heating to 650 °C does not change the CoSi₂ peak intensity for Co coverages higher than 2.5 ML. On the other hand, for $\theta_{\text{Co}} \leq 2.5$ ML the CoSi₂ peak intensity increases further. A possible explanation for this effect would be that the reaction is not complete even at 460 °C for $\theta_{\text{Co}} \leq 2.5$ ML. For all coverages the intensity of the surface peak increases after the last anneal but no further binding-energy shift occurs. We could attribute this intensity increase to Si diffusion on the surface during the formation of the CoSi₂-S surface which takes place after this anneal (compare Sec. III). The observed additional increase of the total intensity supports such an interpretation. The binding energy shift of the surface peak (-0.42 eV) is close to the binding energy shift of the surface peak of the upper dimer atoms on the clean surface (-0.47 eV). Most probably our surface peak contains contributions from disilicide islands and Si pinholes.

This suggestion is supported by the fact that we always observe the (2×1) LEED pattern of the clean Si(100) surface after annealing these Co films to 650 °C (see Sec. III).

Now we could offer another explanation of the above-discussed intensity increase of the CoSi_2 bulk peak at 650 °C for 1.3 ML as being due to a contribution from the second surface peak of the lower dimer atoms, which we cannot resolve.

It is worth noting that at all Co coverages and annealing temperatures we always observe the Si bulk peak (Fig. 5). The mean free path of the 30-eV electrons in CoSi_2 is $\sim 2.0\text{--}2.5$ Å.²⁷ Assuming that our films are complete the thickest one (5-ML Co) is ~ 11 Å thick. Therefore, we should not observe any Si bulk emission if our film was complete. The observation of Si bulk emission means that we never obtain a CoSi_2 film without pinholes. We estimate an upper limit of the area covered by pinholes to be $\sim 17\text{--}27\%$ of the surface. The lowest pinhole area is observed for 2.6-ML Co coverage.

From our Si 2*p* data, we can exclude RT CoSi_2 formation on the Si(100) surface; the Co reaction with Si leads only to the formation of a Co-Si solid solution. It seems that at $\theta_{\text{Co}} \leq 2.5$ ML, CoSi_2 formation needs higher temperatures than at higher coverages and on the Si(111) surface. We attribute this effect to the change of the RT Co diffusion mechanism.⁷ It is understandable that the CoSi_2 formation reaction would be easier if a Co-Si exchange has taken place above 2.5 ML at RT. The CoSi_2 films obtained after annealing contain a considerable amount of pinholes.

VI. Co 3*p* CORE-LEVEL SPECTRA

Figure 6 presents the Co 3*p* spectra of 0.7-ML and 5-ML Co/Si(100) recorded before and after annealing. For these experiments we used a photon energy of 170 eV, which means that the emitted Co 3*p* electrons have a kinetic energy of ~ 100 eV. Therefore we are less surface sensitive, but nevertheless the signal originates from the topmost layers due to the fact that the Co atoms are

near the surface. The lines show the best fits to the experimental data (dots) using the same fitting procedure as in Sec. V. The statistics of the data were not good enough to determine the asymmetry parameter, so it was chosen as zero. The spin-orbit splitting is ~ 1.5 eV, which should be compared with the value for the Ni 3*p* level of ~ 1.6 eV.³⁰ The Lorentzian FWHM is ~ 0.19 eV and the Gaussian width is due to the lower resolution at the higher photon energy ~ 0.6 eV. We fitted all spectra with only one spin-orbit-split peak using the statistical branching ratio of 0.5. It should be noted that Leckey *et al.*²⁹ observed from their Gaussian fits of Co 3*p* levels for monocrystalline CoSi_2 a spin-orbit splitting of 1.38 eV and a branching ratio of 0.44.

From the bottom spectra of Fig. 6 we see the intensity increase with Co coverage. The $3p_{3/2}$ component shifts from 59.8 eV (0.7 ML Co) to 59.4 eV (5 ML Co) binding energy, the value for metallic Co,³¹ which demonstrates the lower coordination of the topmost Co atoms with Si atoms.

The first annealing does not change the 0.7-ML spectrum but causes an intensity reduction and a shift to higher binding energy of the 5-ML spectrum. This suggests negligible Co inward diffusion in the former case in contrast to the latter case. This observation is compatible with the observed Co chemisorption on the topmost layer of the Si(100) surface for $\theta_{\text{Co}} < 0.5$ ML.⁷ In both cases a shift to higher binding energy is observed which means that a reaction has taken place during the anneal. Further annealing to 460 °C and 650 °C leads in both cases to an intensity decrease and to a shift to higher binding energy which reaches ~ 60 eV. The final binding energy is significantly lower than that observed for monocrystalline CoSi_2 (61.65 eV).²⁹ We do not have an explanation for this difference. It should be noted, however, that the Si 2*p* binding energy in CoSi_2 observed in Ref. 29 is higher than ours by 0.5 eV as well. We observed that during CoSi_2 formation the Co 3*p* levels have shifted by ~ 0.6 eV to higher binding energy. A much higher shift (1.6 eV) to higher binding energy has

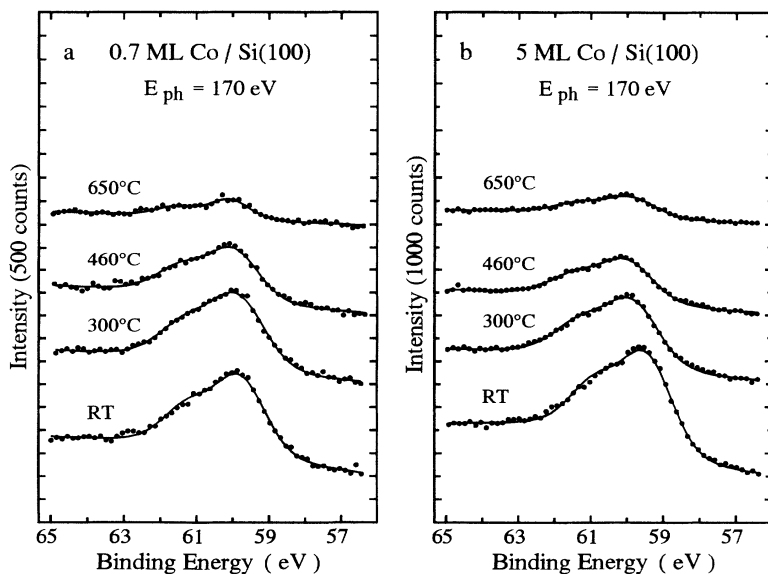


FIG. 6. Co/Si(100), Co 3*p* spectra (a) for $\theta_{\text{Co}} = 0.7$ ML and (b) for $\theta_{\text{Co}} = 5$ ML. The intensity units correspond to the distance between two axes markers.

been observed in the case of NiSi₂ formation^{30,32} and was attributed to changes in the electronic configuration from Ni metal to NiSi₂, becoming atomiclike in the latter case, but not to a charge transfer from Ni to Si as one would expect from the direction of the binding-energy shift in the framework of the simple electrostatic model.¹⁸ A later theoretical study by Lambrecht³³ has excluded final-state effects and observed charge transfer from Si to Ni, the extra charge being *p*-like and producing a negative initial-state shift. The experimentally observed positive binding-energy shift has been explained by a stabilizing Madelung initial-state shift.³³ The different value for Co could mean a weighting of the various contributions to the binding-energy shift. Theoretical calculations are needed to clarify this problem.

From the temperature behavior of the Co 3*p* spectra, we conclude that at RT 0.7-ML Co reacts with the substrate but the reaction is not complete. The reaction to CoSi₂ is not accompanied by significant diffusion (peak intensity does not change up to 300 °C). At higher Co coverages the topmost Co layer reacts less with Si (shift to lower binding energy with increasing coverage) which means that the RT reaction to CoSi₂ is limited to the interface region.

VII. DISCUSSION AND SUMMARY

The Co reaction on Si(100) surfaces was studied here using an *in situ* combination of surface analytical tools. This allowed for a better comparison of the experimental results obtained by the different techniques, and eliminates to a great extent disagreements due to different preparation procedures and experimental conditions.

Our answer to the important question about an eventual RT CoSi₂ formation is definitively negative. Neither the valence-band electronic structure nor the Si and Co core-level data indicate such a reaction. The Co 3*d* and 3*p* binding energy correspond to lower-coordinated Co atoms on the surface even at the lowest coverage of 0.7 ML. In the Si 2*p* core-level spectra we observe the contribution from Co-Si solid solution only. The Co 3*p* intensity data show that at low Co coverages the RT inward Co diffusion is low, which is compatible with the model of Meyerheim, Döbler, and Puschmann⁷ proposing overlayer chemisorption of the first 0.5 ML of Co; this preserves the surface periodicity as we observe by LEED. Additional Co deposition leads to further intensity increase and a shift to lower energy of the Co 3*d* and 3*p* emission in the valence-band spectra and core-level spectra, respectively. The Co-Si peak in the Si 2*p* core-level spectra also grows in intensity. This means that a Co-Si mixed layer covers the surface. The annealing experiments confirm this statement. For all coverages we observed that formation of CoSi₂ takes place only after annealing. This behavior contrasts with the Co/Si(111) reaction, where at least 0.2 ML of Co react to CoSi₂ at RT.^{8,26,27}

We observe above 2.5 ML a rapid change of the RT growth mode, accompanied by the disappearance of the (1 × 1) LEED pattern. Similar results have been attributed to a change of the Co diffusion mechanism from interstitial to site exchange.⁷ We observe for the first time, to our knowledge, a coverage dependence of the

CoSi₂ formation after annealing of the RT deposited films. For $\theta_{\text{Co}} \leq 2.5$ ML annealing even to 460 °C was not enough for completion of the reaction. Only after high-temperature annealing did we get the DOS of bulk CoSi₂ even for θ_{Co} as low as 0.7 ML. Obviously, no complete CoSi₂ layer is possible for such a low θ_{Co} . Therefore, we must accept that islands of CoSi₂ form on the surface during annealing. This statement is supported by the observation that (2 × 1) or (2 × 2) LEED patterns appear after annealing, showing that patches of clean Si(100) surface exist. We cannot estimate the lateral size of the CoSi₂ islands, but from the transition from a (2 × 1) to a *p*(2 × 2) LEED pattern one can infer that their lateral size increases with Co coverage.

The temperature treatment of Co films with $\theta_{\text{Co}} > 2.5$ ML shows that even at 300 °C (460 °C) most (all) of the Co atoms are in the CoSi₂ environment. The observation that for $\theta_{\text{Co}} > 2.5$ ML the silicide formation reaction occurs more easily is compatible with the proposed change of the Co diffusion mechanism.⁷ It is understandable that the silicide formation should be easier if Co atoms occupy Si lattice sites already at RT. The silicide layers which form after 460 °C for $\theta_{\text{Co}} > 4$ ML show a constant Co/Si AES ratio of ~ 0.18 and a *c*(2 × 2) LEED pattern. These data are typical for the Co-rich CoSi₂-C surface.^{6,8} In our Si 2*p* data for the CoSi₂-C surface we observe emission from lower-coordinated Si atoms, which we attribute to the topmost Si layer. Therefore, we reject the Co termination of the CoSi₂-C surface proposed by Chambliss *et al.*⁸ and support a termination with 1 ML Si as proposed by Stalder *et al.*⁹ In contrast to Si(111),²⁷ however, our Si 2*p* data show that we did not succeed in producing pinhole-free CoSi₂-C surfaces on Si(100). From the absence of the (2 × 1) LEED pattern of the clean Si surface at $\theta_{\text{Co}} \geq 3$ ML, we can conclude that the lateral dimensions of the pinholes are at least 3–4 times smaller than the LEED coherence length of ~ 100 Å. Alternatively, the high quality of the *c*(2 × 2) LEED pattern suggests that the dimensions of the CoSi₂ area should be close to the LEED coherence length. Therefore, we observe a tendency for a lateral growth of the CoSi₂ areas with Co coverage but no complete layer could be obtained in this coverage region. Our Si 2*p* data show that the minimum area covered by pinholes is obtained for coverages ~ 2.6 ML, where Yalisove, Tung, and Loretto³ obtained their best templates. We can conclude from our data that we have observed the initial stages of the CoSi₂ grain formation after annealing RT Co films on Si(100) surfaces.

At 650 °C a Si-rich surface with a Co/Si AES ratio of ~ 0.07 appears. This surface is called CoSi₂-S in analogy to Si(111).^{6,9} We observed a *c*(4 × 4) LEED structure of the CoSi₂(100)-S surface but not the (3√2 × √2)*R*45° one, observed earlier.⁹ We cannot explain this difference. Obviously, further investigations are needed to clarify this point.

ACKNOWLEDGMENTS

We acknowledge stimulating discussions with Professor W. Steinmann and experimental help by B. Eisenhut. This work was supported by the German Federal Minister of Research and Technology (BMFT 05 5WMABB 2).

- ¹ H. von Känel, *Mater. Sci. Rep.* **8**, 193 (1992).
- ² C. W. T. Bulle-Lieuwma, A. H. van Ommen, and J. Hornstra, in *Epitaxy of Semiconductor Layered Structures*, edited by R. T. Tung, L. R. Dawson, and R. L. Gunshor, MRS Symposia Proceedings No. 102 (Materials Research Society, Pittsburgh, 1988), p. 377.
- ³ S. Yalisove, R. Tung, and D. Loretto, *J. Vac. Sci. Technol. A* **7**, 1472 (1989).
- ⁴ R. T. Tung and F. Schrey, *Appl. Phys. Lett.* **54**, 9 (1989).
- ⁵ C. W. T. Bulle-Lieuwma, A. H. van Ommen, J. Hornstra, and C. N. A. M. Aussems, *Appl. Phys.* **71**, 2111 (1992).
- ⁶ J. M. Gallego *et al.*, *Surf. Sci.* **239**, 203 (1990).
- ⁷ H. L. Meyerheim, U. Döbler, and A. Puschmann, *Phys. Rev. B* **44**, 5738 (1990).
- ⁸ D. D. Chambliss, T. N. Rhodin, J. E. Rowe, and S. M. Yalisove, *Phys. Rev. B* **45**, 1193 (1992).
- ⁹ R. Stalder, C. Schwarz, H. Sirringhaus, and H. von Känel, *Surf. Sci.* **271**, 355 (1992).
- ¹⁰ F. Hellman and R. T. Tung, *Phys. Rev. B* **37**, 10786 (1988).
- ¹¹ C. A. Schug *et al.*, *Surf. Sci.* **225**, 58 (1990).
- ¹² D. Rieger, R. D. Schnell, W. Steinmann, and V. Saile, *Nucl. Instrum. Methods* **208**, 777 (1983).
- ¹³ D. D. Chambliss, T. N. Rhodin, J. E. Rowe, and H. Shigekawa, *J. Vac. Sci. Technol. A* **7**, 2449 (1989).
- ¹⁴ R. Stalder *et al.*, *J. Vac. Sci. Technol. B* **9**, 2307 (1991).
- ¹⁵ J. J. Yeh and I. Lindau, *At. Data Nucl. Data Tables* **32**, 1 (1985).
- ¹⁶ J. Tersoff and D. R. Hamann, *Phys. Rev. B* **28**, 1168 (1983).
- ¹⁷ C. Pirri, J. C. Peruchetti, G. Gewinner, and J. Derrien, *Phys. Rev. B* **30**, 6227 (1984).
- ¹⁸ F. J. Himpsel *et al.*, *Phys. Rev. B* **38**, 6084 (1988).
- ¹⁹ W. H. Press, B. P. Flannery, S. A. Teukolsky, and W. T. Vetterling, *Numerical Recipes* (Cambridge University Press, Cambridge, 1986).
- ²⁰ S. Doniach and M. Šunjić, *J. Phys. C* **3**, 285 (1970).
- ²¹ U. Gelius *et al.*, *Nucl. Instrum. Methods B* **1**, 85 (1984).
- ²² J. E. Rowe, G. K. Wertheim, and R. T. Tung, *J. Vac. Sci. Technol. A* **7**, 2454 (1989).
- ²³ G. K. Wertheim, in *Photoemission and Absorption Spectroscopy of Solids and Interfaces with Synchrotron Radiation*, Proceedings of the International School of Physics "Enrico Fermi", Course CVIII, Varenna, 1988, edited by M. C. Campagna and L. Rosei (North-Holland, Amsterdam, 1990), p. 237.
- ²⁴ L. I. Johansson *et al.*, *Phys. Rev. B* **43**, 12355 (1991).
- ²⁵ G. J. van Gorp and C. Langereis, *J. Appl. Phys.* **46**, 4308 (1975).
- ²⁶ F. Boscherini, J. J. Joyce, M. W. Ruckman, and J. H. Weaver, *Phys. Rev. B* **35**, 4216 (1987).
- ²⁷ G. Rangelov, P. Augustin, J. Stober, and T. Fauster, *Surf. Sci.* (to be published).
- ²⁸ M. del Giudice, J. J. Joyce, and J. H. Weaver, *Phys. Rev. B* **36**, 4761 (1987).
- ²⁹ R. Leckey *et al.*, *J. Vac. Sci. Technol. A* **6**, 63 (1988).
- ³⁰ A. Franciosi, J. H. Weaver, and F. A. Schmidt, *Phys. Rev. B* **26**, 546 (1982).
- ³¹ D. A. Shirley *et al.*, *Phys. Rev. B* **15**, 544 (1977).
- ³² O. Bisi, L. W. Chiao, and K. N. Tu, *Phys. Rev. B* **30**, 4664 (1984).
- ³³ W. R. L. Lambrecht, *Phys. Rev. B* **34**, 7421 (1986).